*Polish Journal of Chemical Technology, 19, **1**, 27—33, 10.1515/pjct-2017-0004*

Cytotoxicity and genotoxicity of GO-Fe_3O_4 hybrid in cultured mammalian cells

Magdalena Jedrzejczak-Silicka

West Pomeranian University of Technology, Szczecin, Laboratory of Cytogenetics, Doktora Judyma 6, 71-466 Szczecin, Poland
Corresponding author: e-mail: mjedrzejczak@zut.edu.pl

The study was aimed at investigating the effect of the Fe_3O_4 hybrid deposited on graphene oxide (GO-Fe_3O_4) on the relative viability and DNA integrity. The properties of the GO-Fe_3O_4 hybrid were analyzed using a transmission electron microscopy (TEM), X-ray diffraction technique (XRD) and thermal gravimetric method (TGA), while the efficiency of graphene oxide covalent functionalization with iron oxide nanospheres was determined by Fourier transform infrared spectroscopy (FT-IR). L929 and MCF-7 cell lines were selected to analyze the biocompatibility of GO-Fe_3O_4 nanoparticles. The hybrid was tested using WST-1 and LDH leakage assays. DNA integrity was analyzed by agarose gel electrophoresis and micronucleus assay was performed to examine chromosomal damage in the exposed cell lines. The tested GO-Fe_3O_4 hybrid did not significantly reduce cell metabolism of L929 cells. GO-Fe_3O_4 hybrid particles only slightly affected the integrity of cell membranes. DNA integrity and micronucleus assays did not indicate genotoxicity of the hybrid.

Keywords: GO-Fe_3O_4 hybrid, relative viability, DNA fragmentation, micronucleus assay, genotoxicity.

INTRODUCTION

Graphene oxide (GO) is one of the most popular graphene derivatives. Its unusual properties (e.g., electrical, optical, thermal or mechanical) are mainly determined by the chemical structure composed of sp3 carbon domains surrounding the sp2 carbon domain[1]. Another important characteristics of GO is a structure with a large specific surface area. These unique properties make GO an ideal carrier of many various molecules (e.g., drugs, fluorescent dyes, photosensitizers or ferromagnets), and for this reason, many recent studies have focused on GO as a drug delivery system, also suitable for the thermally-responsive therapy using the GO platform for loading magnetic nanoparticles[2, 3, 4].

Recently, various metal oxides (e.g. ZnO, AgNPs, TiO_2, Fe_3O_4) have been manufactured and incorporated into different products (e.g., plastics, glass, textiles, reinforce, pigments, medical devices and many others) to expand their properties and broaden product's applications[5, 6]. It was possible thanks to the unique capabilities of metal oxides, such as catalytic, antimicrobial, antioxidant, optoelectronic or ferromagnetic characteristics[5, 6]. It was also found that some of those attractive metal oxides can be cyto-and/or genotoxic and induce cellular changes resulting in a disruption of mitochondrial membrane integrity, DNA fragmentation and cell death. Lately, several studies have focused on Fe_3O_4 nanoparticles due to its magnetic properties that can be successfully applied in the medical sector. The Fe_3O_4 nanoparticles were used for GO-Fe_3O_4 preparation for different applications; for example, GO-Fe_3O_4 with an anticancer drug, as an alternative form of cancer treatment, reduced GO-Fe_3O_4 NPs used as a magnetic resonance contrast agent or GPO-do-Fe_3O_4 nanoparticles (Fe_3O_4 nanoparticles covalently bonded to graphene oxide (GPO) through dopamine (do)) synthesized for electro-magnetic devices[7, 8]. Due to the immense potential of GO-Fe_3O_4 application in biomedical and other fields, those recent studies have focused on the potential cytotoxicity and genotoxicity of this type of hybrid[8]. An important aspect of those studies is to find out as much as possible about the interactions between NPs and biological systems. These analyses, including plasma membrane damage, induction of oxidative stress, impairment of mitochondrial activity and DNA damage bioassays should complement a wide and proper physico-chemical characteristics of NPs[9].

Advances in understanding the relationship between physicochemical parameters and potential cytotoxicological effects of synthesized hybrid need to clarify and should correspond to mainstream nanotechnology and its wide range of biomedical applications. Thus, the aim of the study was to evaluate the cellular response of L929 and MCF-7 cell lines to 48-hour incubation with graphene oxide nanosheet/Fe_3O_4 nanoparticles (GO-Fe_3O_4).

EXPERIMENTAL

Preparation of graphene oxide-Fe_3O_4 nanoparticle hybrids

Synthesis of graphene oxide

In order to produce graphene oxide (GO), modified Hummers method has been used. Briefly, 1 g of graphite and 6 g of $KMnO_4$ were placed together in a round-bottom flask. A mixture of concentrated H_2SO_4 (120 ml) and H_3PO_4 (15 ml) was slowly poured into the flask with powders, followed by heating to 50°C and stirring for 12 hours. After cooling down to the room temperature, 1 ml of H_2O_2 (30%) was slowly added. The mixture was purified by sequential washing and centrifugation with water, HCl aqueous solution (1:3) and ethanol. The product was vacuum dried at 60°C. The whole procedure has been described in details by Marcano et al.[10].

Synthesis of magnetite nanospheres (Fe_3O_4)

To synthesize iron oxide nanospheres, 20 ml of ethylene glycol (EG) and 400 mg of iron oxide precursor – iron chloride ($FeCl_3$) were mixed together in a glass beaker followed by ultrasonication until the homogeneous dispersion was received. In the next step, sodium acetate (5.0 g) was added to the mixture. After ultrasonication, the dispersion was transferred into the sealed teflon-lined

stainless steel autoclave for 6 h at 200°C. The suspension was separated with a magnet and washed thoroughly with ethanol and water. The obtained product was vacuum dried in 100°C.

Synthesis of graphene oxide – Fe_3O_4 (GO-Fe_3O_4)

In order to produce GO-Fe_3O_4 the glycine was used as a linker. Firstly, 20 mg of Fe_3O_4 nanospheres was dispersed in water (0.5 $mgml^{-1}$) and ultrasonicated until the homogeneous dispersion was obtained followed by functionalization with glycine in order to attach $–NH_2$ groups to its surface. 20 mg of graphene oxide sample was exfoliated in 60 ml H_2O by the ultrasonication to produce a homogeneous graphene oxide water-based suspension. Then, the carboxylic groups on the graphene oxide surface were activated with 8 mg of N-hydroxysuccinimide (NHS) and 10 mg of 1-(3-dimethylaminopropy--l)-3-ethylcarbodiimide (EDC). The mixture of modified iron oxide and graphene oxide was stirred for 2 h. The obtained product was centrifuged, washed several times with water and ethanol and dried in 100°C.

Characterization of synthesized nanocomposite

The morphology of graphene flakes covered with GO-Fe_3O_4 nanospheres, size and distribution of the magnetite nanoparticles was examined using a high-resolution transmission electron microscopy (HRTEM) (FEI Tecnai F30, Frequency Electronics Inc.). X-ray diffraction technique (XRD) ($K_{\alpha 1}$ = 1.54056 A, X'Pert Philips Diffractometer, PANanalytical) was used to investigate the crystal structure of the prepared samples and to estimate the average size of magnetite nanoparticles. The composition of the samples was analyzed by thermal gravimetric method (TGA) (SDT Q600 Simultaneous TGA/DSC, TA Instruments) under an air flow of 100 ml/min and a heating rate of 5°C/min. The efficiency of the covalent functionalization of graphene oxide with iron oxide nanospheres was determined by Fourier transform infrared spectroscopy (FT-IR) (Nicolet 6700 FT–IR Spectrometer, Thermo Scientific). The spectra obtained with FT-IR demonstrated successful functionalization of GO with Fe_3O_4 via a covalent bond.

Cell culture conditions

Two cell lines – mouse L929 fibroblasts and MCF-7 human breast adenocarcinoma – were seeded on 96-well microplates (Corning Inc.) at a density of 7.4 x 10^3 per well (for WST-1, LDH assays) and in T25 flasks (Sarstedt) at a density of 7 x 10^5 per flask (for genotoxicity assays) in standard culture conditions at 37°C, 5% CO_2 and were cultured 95% humidity. Complete DMEM (Dulbecco's Modified Eagle Medium, High Glucose, Gibco) supplemented with 10% heat-inactivated fetal bovine serum (Sigma-Aldrich), 2 mM L-glutamine (Sigma-Aldrich) and 0.4% streptomycin-penicillin (Sigma-Aldrich) was used to maintain cell cultures. Cell lines were monitored with a Nikon TS-100 microscope (NIS Elements F Pakage, Nikon). After a 24–h incubation period, the GO-Fe_3O_4 nanocomposite was added to the cell culture at final concentrations of 0.0, 3.125, 6.25, 12.5, 25.0, 50.0, 100.0 $\mu g\ ml^{-1}$ in the culture medium. Cell lines were incubated with the hybrid for 48 h.

Relative mitochondrial activity

Firstly, the relative mitochondrial activity of L929 and MCF-7 cell lines after 48-h incubation with the hybrid was tested using the WST-1 Cell Proliferation Reagent (Roche Applied Science). The WST-1 assay is based on the mechanism of reduction reactions of WST-1 salt catalyzed by cellular dehydrogenases from metabolically active cells[11]. The number of metabolically active cells is proportional to the amount of the reduction product. The WST-1 solution (20 μl) was added to each well and incubated for additional 60 minutes at 37°C. After incubation, the absorbance was recorded at 450 nm (with a reference wavelength of 630 nm), according to the manufacturer's instructions, on a Sunrise Absorbance Reader (Sunrise, Tecan). Cells maintained in a complete DMEM medium without adding the tested samples were used as a control. The interaction between nanomaterials and WST-1 reagents was also determined. All the experiments were conducted in triplicate. The relative cell viability was calculated using the following formula (1):

$$\text{Relative viability} = \frac{\{\text{OD value}\}_{nanocomposite} - \{\text{OD value}\}_{control}}{\{\text{OD value}\}_{control}} \quad (1)$$

where OD is optical density.

Lactate dehydrogenase leaking assay

The cytotoxicity of GO-Fe_3O_4 exposure was determined using the LDH CytoTox 96® Non-Radioactive Cytotoxicity Assay (Promega). The lactate dehydrogenase (LDH) leaking assay measures lactate dehydrogenase enzyme released due to the cellular membrane damage. The number of lysed cells is proportional to the amount of formazan converted from the tetrazolium salt. Optical density values were measured at 490 nm using a microplate spectrophotometer (Sunrise Absorbance Reader, Tecan). The interaction between different concentrations of the nanocomposite in cell culture medium and LDH assay components was carried out in the absence of cells. The percentage of LDH released (cytotoxicity) after 48-hour exposure was calculated using the formula (2):

$$\%\text{LDH released} = \frac{\text{A490 nm of treated and untreated cells-A490 nm of control}}{\text{A490 nm of maximum of untreated cells-A490 nm of control}} \text{ x100} \quad (2)$$

where A is absorbance.

DNA fragmentation assay

Nuclear DNA fragmentation can be used for the detection of the apoptotic effect. After 48 hours of treatment, L929 and MCF-7 cells were harvested by scraping in 1xDPBS (Gibco) and pelleted by centrifugation at 1000 rpm. Then, genomic DNA was extracted from cell cultures using silica microcolumns (Genomic Mini Kit, A&A Biotechnology), according to the manufacturer's protocol. The extracted DNA was suspended in 200 μl of Tris-EDTA buffer. The quantity of DNA was determined fluorometrically using Quant-iT™ DNA BR Assay Kit (Invitrogen) and Qubit fluorometer (Invitrogen). The integrity of genomic DNA was analyzed electrophoretically on 1% agarose gel (Basica, Prona) prepared in 1xTBE buffer (Chempur) stained with 1.0 μM ethidium bromide (Aplichem). Equal amounts of DNA isolates were loaded and separated by horizontal electrophoresis (80 V, 400 mA, 60 minutes) and visualized at 312 nm using UV

transilluminator (Vilber Lourmat). For reference, 1 kb DNA Ladder (GeneRuler, Thermo Scientific) was used.

Micronucleus assay

Micronucleus assay was also performed to examine chromosomal damage in the exposed cell lines. The cells plated on T25 flasks (Sarstedt) were exposed to six doses (3.125–100.0 μg ml^{-1}) of the nanocomposite. Treatment time was 48 h. Cytochalasin B (15 μg ml^{-1}, Sigma-Aldrich) was added to induce binucleation of dividing cells. Positive controls were obtained by exposing the cells to mitomycin C (5 μg ml^{-1}, Sigma-Aldrich). The untreated control was also included in a 48-hour incubation period. After incubation, the cells were harvested, transferred to 15 ml tubes (Sarstedt) and centrifuged at 1200 rpm for 10 min. The supernatant was then discarded and the cells were resuspended in a hypotonic buffer (0.075 M KCl, Chemland) and incubated for 5 min at 37°C. Next, the cells were centrifuged at 1200 rpm for 10 min and the supernatant was discarded by pipetting and the cells were fixed with 2 ml of Carnoy's fixative (methanol/acetic acid, 3:1, Chemland). Finally, the cells were spread on microscope slides and stained with Giemsa solution (Chempur) for 8–12 min. The presence of MN in each slide was scored (1000 cells) using a Zeiss Axiolab microscope. Data presented for MN are the mean of two slides.

The cytokinesis-block proliferation index (CBPI) was calculated from 100 cells per sample[12, 13] using the formula (3):

$$\text{CBPI} = \frac{(\text{no. mononucleate cells}) + 2(\text{no. mononucleate cells}) + 3(\text{no. multinucleated cells})}{\text{total no. of cells}} \quad (3)$$

Statistical analysis

The data collected in this study are given as the mean values ± standard deviation (SD). All results were compared using the Student's t-test. Differences were considered significant at $P<0.05$. Statistical analyses were performed using Statistica 12.5 (StatSoftInc., Tulsa, OK, USA).

RESULTS AND DISCUSSION

Transmission electron microscopy (TEM) was employed in order to investigate the morphology of the hybrid. Representative TEM images of the GO-Fe_3O_4 hybrid are shown in Figure 1. The observations revealed the spherical shape of magnetite nanospheres. A histogram presenting diameter distribution of Fe_3O_4 nanospheres (Fig. 1C) shows that the diameter of the nanospheres is in the range of 70–230 nm. Images 1A and 1B present a heterogeneous coverage of graphene flakes with nanospheres.

X-ray diffraction (XRD) was applied to study the crystal structure of the material. XRD pattern of the GO-Fe_3O_4 hybrid is presented in Figure 1D. The spectrum of GO-Fe_3O_4 is dominated by intense and narrow peaks indexed as planes (220), (311), (400), (422), (511) and (440). The data obtained are consistent with the standard XRD data for magnetite (ICSD 65339).

Thermal gravimetric analysis was used to determine sample composition. Figure 1E demonstrates the thermogravimetric curve of GO-Fe_3O_4 nanosphere hybrids heated in the air to 700°C. The weight loss observed at 100°C corresponded to decomposition of physically adsorbed water. The following weight loss occurred between 150°C and 300°C and was associated with decomposition of oxygen-containing functional groups, which meant that graphene oxide did not undergo a complete reduction during magnetite attachment. The next weight loss could be assigned to the bulk pyrolysis of the carbon skeleton. TG curve of the hybrid indicated that the amount of loaded Fe_3O_4 was ca. 34 wt%.

The efficiency of the covalent functionalization of graphene oxide with iron oxide nanospheres was performed using Fourier transform infrared spectroscopy. The presented spectra provide evidence for successful GO functionalization with Fe_3O_4 via the covalent linkage. Figure 1F presents FTIR spectra of GO-Fe_3O_4. The FTIR absorption spectrum of GO-Fe_3O_4 was dominated by peaks at 794 cm^1 and 1118 cm^{-1}. The reduction of Fe_3O_4 to nanoscale dimension resulted in a higher surface bond force constant and a shift to higher bands of IR spectra[14]. Several new peaks occurred after functionalization: peak at 1580 cm^{-1} was derived from C-N bonding and 3421 cm^{-1} corresponded to the N-H bond[15]. Both of them are characteristic of amide bonding[16]. The peak at 1700 cm^{-1} originated from C=O bonding from the carboxyl group of graphene oxide or from amide bonding[15].

First, this study determined the effect of the GO-Fe_3O_4 hybrid on the cellular metabolism of L929 and MCF-7 cell lines after 48 h incubation with the hybrid using the WST-1 Cell Proliferation Reagent. The analysis of L929 cells incubated with the GO-Fe_3O_4 hybrid showed that this type of nanomaterial did not affect cell viability in a dose-dependent manner (Fig. 2A). L929 fibroblasts exposed to the GO-Fe_3O_4 hybrid showed the lowest OD values of cells incubated with the tested nanomaterial at 3.125–6.25 μg ml^{-1} concentrations (no statistically significant differences were found). Higher values were recorded when the cells were co-incubated with the hybrid material at a concentration range of 50.0–100.0 μg ml^{-1}. The cells incubated with the GO-Fe_3O_4 hybrid at a concentration of 12.5 μg ml^{-1} exhibited the highest cell mitochondrial metabolism. Moreover, the cytotoxicity of GO-Fe_3O_4 exposure was determined using the LDH CytoTox 96® Non-Radioactive Cytotoxicity Assay. The highest LDH leakage was observed at a dose of 50.0 μg ml^{-1} ($P<0.05$). A lower cytotoxic effect on LDH leakage was recorded for 3.125 and 6.25 μg ml^{-1} ($P<0.05$) hybrid concentrations (Fig. 2B).

Similarly, the influence of the GO-Fe_3O_4 hybrid on MCF-7 was evaluated using WST-1 and LDH leakage assays. The relative mitochondrial activity of MCF-7 cells, in the contrast to L929 cells, was affected by the tested hybrid in a dose-dependent manner. This correlation was clearly noticeable for the high nanomaterial concentration >12.5 μg ml^{-1} (Fig. 2A). The GO-Fe_3O_4 hybrid most highly reduced the mitochondrial activity at concentrations ranging from 25.0 to 100.0 μg ml^{-1} ($P<0.05$). The viability of MCF-7 decreased approx. by 50% compared to the free-growing cells. The data obtained from LDH assay showed that the effect of the GO-Fe_3O_4 hybrid on cell membrane integrity was not dose-dependent. The highest LDH leakage was observed

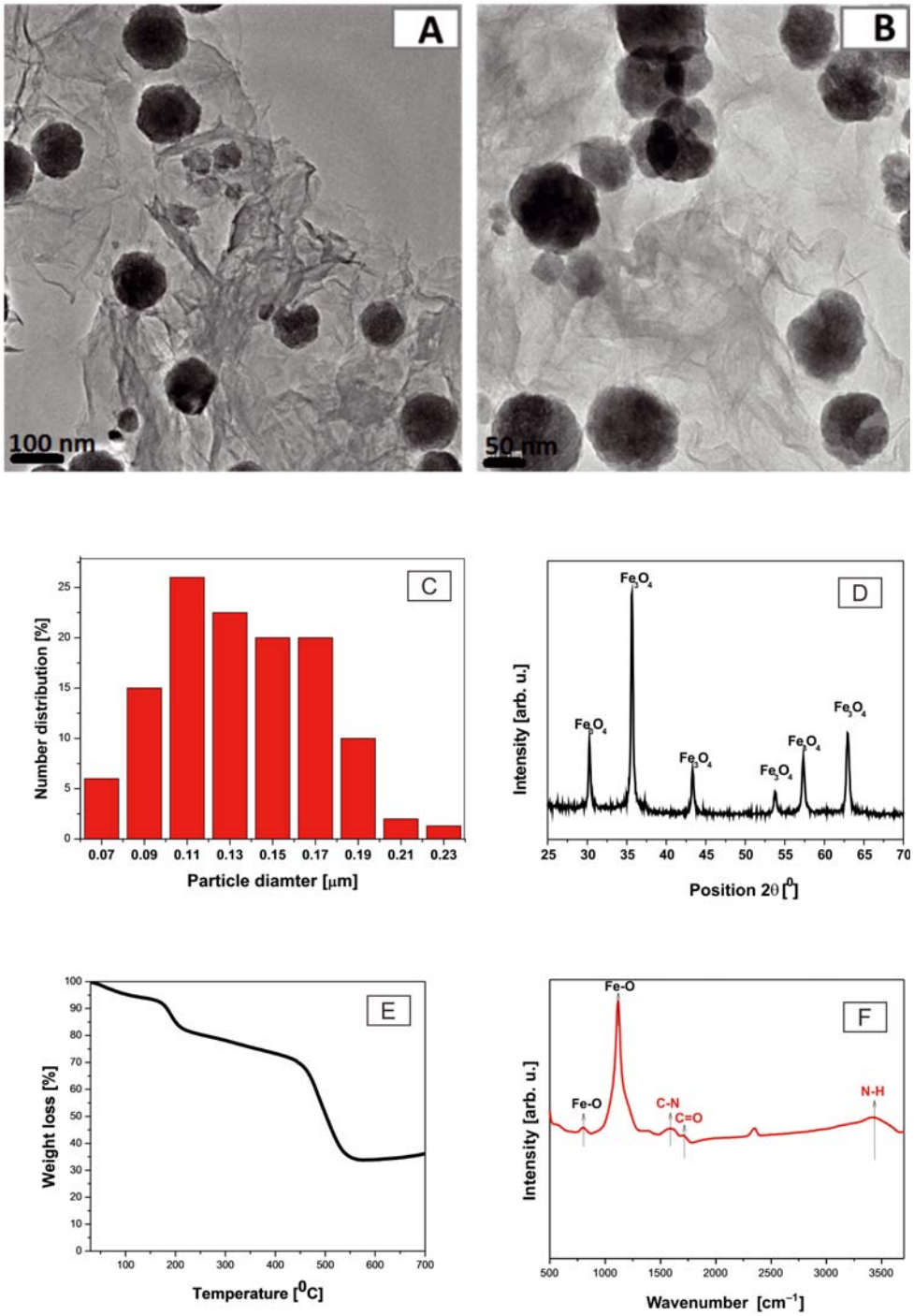

Figure 1. TEM image of GO-Fe_3O_4 hybrid (A, B); diameter distribution of magnetite nanospheres (C); XRD spectra of GO-Fe_3O_4 (D); TG curve of GO-Fe_3O_4 (E); FTIR spectrum of GO-Fe_3O_4 (F)

at a dose of 12.5 μg ml^{-1} (approx. 5% of LDH leakage was recorded for this concentration, $P<0.05$) (Fig. 2B).

Comparison of the result showed that the mitochondrial metabolism of the MCF-7 cell line was more affected in the presence of the GO-Fe_3O_4 hybrid than the L929 cell line. It was also noted that the LDH leakage response to hybrid particles was different in both cell lines. Although the relative viability of MCF-7 cells was lower and the LDH release and membrane integrity was less affected during exposure to GO-Fe_3O_4. Opposite results were obtained for L929 cells, with a higher mitochondrial activity, but also higher LDH release. These findings correspond to previous studies on the L929 cell line performed by Urbas et al.[1, 15] where the biocompatibility of the GO-Fe_3O_4 hybrid was higher than of GO and Fe_3O_4 separately[1]. The relative viability of HeLa cell line treated with the GO-Fe_3O_4 hybrid for 24 hours was higher[17] in comparison to the results obtained in the MCF-7 *in vitro* model.

The DNA laddering technique provides a valuable opportunity to analyze endonuclease cleavage products of the apoptosis process that can be caused by endogenous reactive oxygen species (ROS), errors occurring during the replication or recombination processes or/and environmental toxicants[6, 18]. The damaging effect of the GO-Fe_3O_4 hybrid in L929 and MCF-7 cell cultures was evaluated using the aforementioned method. The integrity of genomic DNA extracted from cell lines exposed to different GO-Fe_3O_4 doses was confirmed by agarose gel electrophoresis. The analyzed hybrid did not induce DNA damage after a 48-hour treatment. High molecular weight DNA extracted from the treated cell cultures was

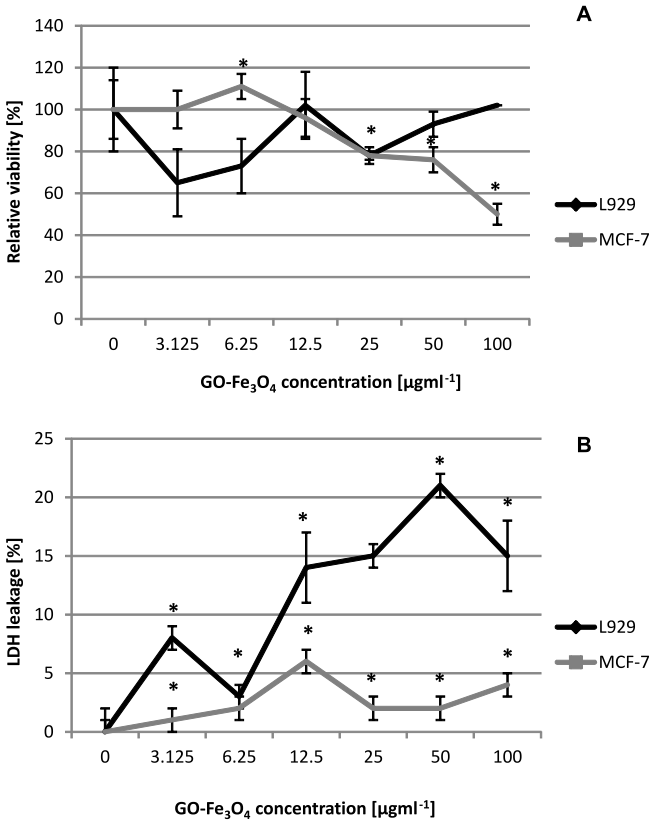

Figure 2. Relative viability of L929 and MCF-7 exposed to GO-Fe_3O_4 hybrid (A); percentage values of LDH release after 48-hour exposition to GO-Fe_3O_4 to hybrid (B). Bars represent standard deviation and asterisk indicates statistically significant difference ($P<0.05$)

visualized at 312 nm using UV transilluminator (Fig. 3). All DNA isolates from both cell lines incubated with different concentrations of the hybrid did not exhibit any DNA fragmentation. Similarly, the negative control set also contained intact DNA visible as a single band on an agarose gel.

It was suggested by Javed et al.[19] that the genotoxic potential could be correlated with the decomposition of mitochondrial membrane potential due to oxidative stress and apoptotic DNA fragmentation[6]. In the current study, the tested GO-Fe_3O_4 hybrid did not affect DNA integrity and did not confirm the induction of apoptosis in L929 and MCF-7 cultures. However, depending on the type of *in vitro* cellular model, the results of WST-1 and LDH assays displayed different tendency in cellular response. The minimal impact of GO-Fe_3O_4 hybrid on mitochondrial metabolism and membrane integrity was recorded in case of L929 culture. The MCF-7 cell line was more susceptible to hybrid nanoparticles, due to higher mitochondrial activity reduction (Fig. 2). In the study presented by Urbas et al.[1] two types of GO-Fe_3O_4 nanocomposites samples (N-GO-Fe_3O_4 with narrower size distribution – 1–3 μm; B-GO-Fe_3O_4 with board size distribution – 0.5–7 μm synthesized by other experimental method described here[1]) were analyzed in the context of its biocompatibility. The cited results emphasize that both tested nanocomposites displayed low cytotoxic activity in L929 cell cultures, with the lower mitochondrial activity registered for 100 μg ml^{-1} of N-GO-Fe_3O_4[1]. Moreover, the result obtained in the presented study are in agreement with the other study described by Urbas et al[15]. The exposition of L929 fibroblasts to GO-Fe_3O_4 hybrid nanoparticles did not evoke high reduction of mitochondrial metabolism (data obtained from WST-1 assay). The verification of the results obtained from WST-1 assays showed that the highest concentration of GO-Fe_3O_4 hybrid in the range of 50.0–100.0 μg ml^{-1} exhibit lactate dehydrogenase (LDH) leakage (approx. 20% of LDH leakage) and the relative viability level determined by neutral red uptake (NRU) assay decreased approx. by 20% compared to the free-growing cells[15]. This comparison suggests slightly better biocompatibility of GO-Fe_3O_4 nanocomposites evaluated on the base of L929 cell culture analysis. In contrast, the results obtained in the studies focusing on AgNPs[6] or ZnO NPs[5] induced cell death with DNA fragmentation – one of two apoptosis hallmarks. AgNPs also caused (in MDA-MB-231 cell cultures) the disruption of cellular function, loss of membrane integrity, which, consequently, led to programmed cell death[6].

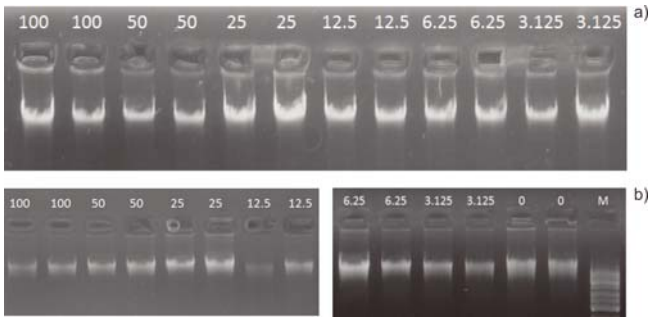

Figure 3. DNA fragmentation analysis. DNA extracted from L929 cells (A); DNA of MCF-7 cells (B) treated with different concentration of GO-Fe_3O_4 hybrid (μg ml^{-1}). Lane M: 1 kB DNA Ladder

The GO-Fe_3O_4 hybrid did not increase the frequency of micronucleated cells in any of the tested doses in both cell lines analyzed compared with the negative control (Fig. 4A). The 48-hour treatment resulted in the highest number of cells with micronucleus at a concentration of 6.25 μg ml^{-1} for MCF-7 and L929 cells, with the highest value (approx. 4% of cells with MN in comparison to the control sample) recorded in MCF-7 cells. The second peak for MN cells was observed at 25 μg ml^{-1} and was approx. 2% for the MCF-7 cell line and 1.2% for L929 cells. The mechanism of DNA-nanoparticles interaction is not well explained. It is stated that particle size and charge may be crucial not only for oxidative stress induction and membrane disruption evoked by mechanical stress, but also for the ability to cross the nuclear envelope and direct interactions with DNA. Small particles seem to be able to enter cells and reach the nucleus of interphase cells. During mitosis, when the nuclear envelope disappears, nanoparticles may easily enter the nucleus and directly interact with genomic DNA or mitotic apparatus[13, 20]. In addition, Lindberg at al.[13] found that the exposure time and concentration of NPs might also affect the capability to reach the nucleus and direct interactions with DNA. The micronucleus analysis can be difficult to perform after the GO-Fe_3O_4 hybrid treatment, as the tested material can cover the slides, especially when 25.0–100.0 μg ml^{-1} doses are used in the experiment. According to the observations

demonstrated by Lindberg et al.[13], higher doses of NPs (e.g., 80.0, 100.0 μgml^{-1}) could be evaluated after 48-h or 72-h incubation periods.

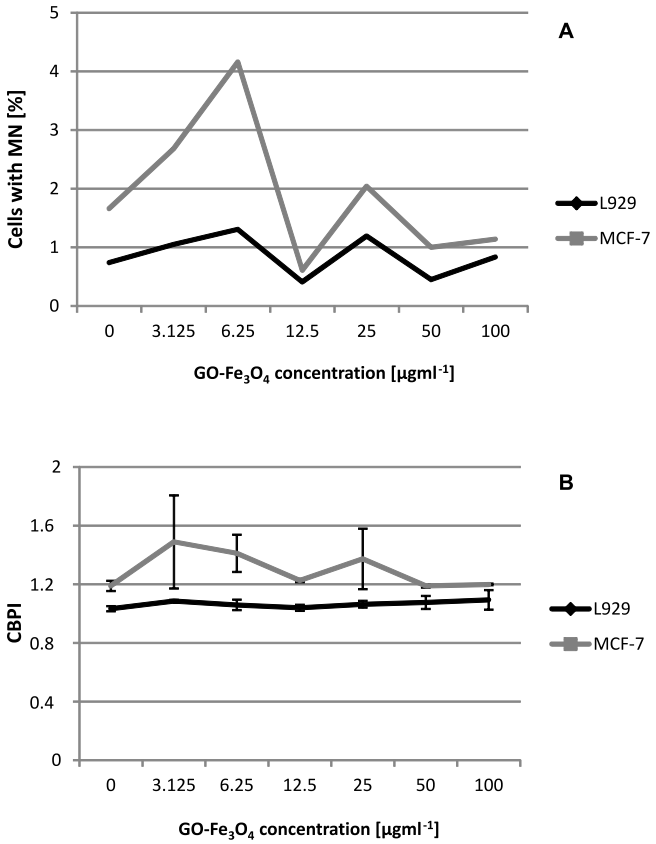

Figure 4. The effect of GO-Fe_3O_4 hybrid on MN frequency in L292 and MCF-7 cells (A); CBPI in L929 and MCF-7 cells exposed to different GO-Fe_3O_4 concentrations after 48 h of incubation (B). Bars represent standard deviation

The evaluated CBPIs were not affected in a dose-dependent manner (Fig. 4B), but a higher CBP index was recorded for the MCF-7 cell line, which was consistent with the results obtained in the MN assay, i.e., higher MN and CBPI values were recorded at two concentration tested, 6.25 and 25 μg ml^{-1} (Fig. 4B, with no statistically significant differences). The CBPI indicated no inhibition of L929 cell proliferation in none of the tested doses of hybrid NPs. The CBP index for MCF-7 cells was higher in comparison to the L929 cell culture, but it reached slightly lower values at concentrations ranging from 50.0 to 100.0 μg ml^{-1} (with no statistically significant differences).

CONCLUSIONS

In summary, it can be concluded that the tested GO-Fe_3O_4 hybrid showed good biocompatibility and did not significantly reduce cell metabolism in the case of L929 cell line. GO-Fe_3O_4 hybrid particles only slightly affected the cell membrane integrity. DNA integrity and micronucleus assays did not indicate hybrid genotoxicity. Therefore, the presented hybrid nanoparticles could potentially be utilized in the evaluation of alternative systems for hyperthermia treatment.

ACKNOWLEDGEMENT

The authors are grateful for the financial support of the National Science Centre within the OPUS program (UMO-2011/03/B/ST5/03239).

LITERATURE CITED

1. Urbas, K., Aleksandrzak, M., Jedrzejczak, M., Jedrzejczak, M., Rakoczy, R., Chen, X. & Mijowska, E. 2014. Chemical and magnetic functionalization of graphene oxide as a route to enhance its biocompatibility. *Nanoscale Res. Lett.* 9, 656. DOI: 10.1186/1556-276X-9-656.
2. Lim, H.M., Huang, N.M., Lim, S.S., Harrison, I. & Chia, C.H. 2011. Fabrication and characterization of graphene hydrogel via hydrothermal approach as a scaffold for preliminary study of cell growth. *Int J Nanomed.* 6, 1817–1823. DOI: 10.2147/IJN.S23392.
3. Wang, K., Ruan, J., Song, H., Zhang, J., Wo, Y., Guo, S. & Cui, D. 2011. Biocompatibility of graphene oxide. *Nanoscale Res. Lett.* 6, 8–16. DOI: 10.1007/s11671-010-9751-6.
4. Balandin, A.A. (2011). Thermal properties of graphene and nanostructured carbon materials. *Nat. Mater.* 10, 569–581. DOI: 10.1038/nmat3064.
5. Chung, I.M., Rahuman, A.A., Marimuthu, S., Kirthi, A.V., Anbarasan, K. & Govindasamy, R. 2015. An investigation of the cytotoxicity and caspase-mediates apoptotic effect of green synthesized zinc oxide nanoparticels using *Eclipta prostrata* on human liver carcinoma cells. *Nanomaterials* 5, 1317–1330. DOI: 10.3390/nano5031317.
6. Gurunathan, S., Raman, J., Malek, S.N.A., John, P.A. &Vikineswary, S. 2013. Green synthesis of silver nanoparticles using *Ganoderma neo-japonicum* Imazeki: a potential cytotoxic agent against breast cancer cells. *Int. J. Nanomed.* 8, 4399–4413. DOI: 10.2147/IJN.S51881.
7. Bai, L.Z., Zhao, D.L., Xu, Y., Zhang, J.M., Gao, Y.L., Zhao, L.Y., Tang, J.T. 2012. Inductive heating property of graphene oxide-Fe_3O_4 nanoparticels hybrid in an AC magnetic field for localized hyperthermia. *Mater. Lett.* 68, 399–401. DOI: 10.1016/j.matlet.2011.11.013.
8. Yang, J.H., Ramaraj, B. & Yoon, K.R. 2014. Preparation and characterization of superparamagnetic graphene oxide nanohybrids anchored with Fe_3O_4 nanoparticles. *J. All. Compd.* 583, 128–133. DOI: 10.1016/j.jallcom.2013.08.152.
9. Lammel, T., Boisseaux, P., Fernández-Cruz, M.L., Navas, J.M. 2013. Internalization and cytotoxicity of graphene oxide and carboxyl graphene nanoplatelets in the human hepatocellular carcinoma cell line Hep G2. *Part Fibre Toxicol* 10, 27. DOI: 10.1186/1743-8977-10-27.
10. Marcano, D.C., Kosynkin, D.V., Berlin, J.M., Sinitskii, A., Sun, Z., Slesarev, A., Alemany, L.B., Lu, W. & Tour, J.M. 2010. Improved synthesis of graphene oxide. *ACS Nano* 4, 4806. DOI: 10.1021/nn1006368.
11. Johnsen, A.R., Bendixen, K. & Karlson, U. 2002. Detection of microbial growth on polycyclic aromatic hydrocarbons in microtiter plates by using the respiration indicator WST-1. *Appl. Environ. Microbiol.* 68, 2683–2689. DOI: 10.1128/AEM.68.6.2683-2689.2002.
12. Surrallés, J., Xamena, N., Creus, A., Catalán, J., Norppa, H., Marcos, R. 1995. Induction of micronuclei by five pyrethroid insecticides in whole-blood and isolated human lymphocyte cultures. *Mutat Res.* 341, 169–184. DOI: 10.1016/0165-1218(95)90007-1.
13. Lindberg, H.K., Falck, G.C.M., Suhonen, S., Vippola, M., Vanhal, E., Catalán, J., Savolainen, K. & Norppa, H. 2009. Genotoxicity of nanomaterials: DNA damage and micronuclei induced by carbon nanotubes and graphite nanofibres in human bronchial epithelial cells in vitro. *Toxicol Lett.* 186, 166–173. DOI: 10.1016/j.toxlet.2008.11.019.

14. Mornet, S., Vasseur, S., Grasset, F. & Duguet, E. 2014. Magnetic nanoparticle design for medical diagnosis and therapy. *J. Mater. Chem*. 14, 2161–2175. DOI: 10.1039/B402025A.
15. Urbas, K., Jedrzejczak-Silicka, M., Rakoczy, R., Zaborski, D. & Mijowska, E. 2016. Effect of GO-Fe_3O_4 and rotating magnetic field on cellular metabolic activity of mammalian cells. *J. Biomater. Appl.* 30, 1392–406. DOI: 10.1177/0885328216628762.
16. Dobson, J. 2006. Magnetic nanoparticles for drug delivery. *Drug. Dev. Res.* 67, 55–60. DOI: 10.1016/S1748-0132(07)70084-1.
17. Chen, W., Yi P., Zhang, Y., Zhang, L., Deng, Z., Zhang, Z. 2011. Composites of aminodextran-coated Fe_3O_4 nanopartilces and graphene oxide for cellular magnetic resonance imaging. *ACS Appl. Mater. Interf.* 3. 4085–4091. DOI: 10.1021/am2009647.
18. AshaRani, P.V., Hande, M.P. & Valiyaveettil, S. 2009. Anti-proliferative activity of silver nanoparticles. *BMC Cell. Biol.* 10, 65. DOI: 10.1186/1471-2121-10-65.
19. Javed, M., Saquib, Q., Azam, A. & Naqvi, S.A.H. 2009. Zinc oxide nanoparticels-induced DNA damage in human lymphocytes. *Int. J. Nanopart.* 2, 402–415. DOI: 10.1504/IJNP.2009.028775.
20. Kazmirova, A., Magdolenova, Z., Barancokova, M., Staruchova, M., Volkovova, K. & Dusinksa, M. 2012. Genotoxicity testing of PLGA-PEO nanoparticles in TK6 cells by the comet assay and the cytokinesis-block micronucleus assay. *Mutat Res.* 748, 42–47. DOI: 10.1016/j.mrgentox.2012.06.012.